

# Open-loop and closed-loop control of posture: A random-walk analysis of center-of-pressure trajectories

J.J. Collins, C.J. De Luca

NeuroMuscular Research Center and Department of Biomedical Engineering, Boston University, 44 Cummington St., Boston, MA 02215, USA

Received: 5 May 1992 / Accepted: 21 December 1992

**Abstract.** A new conceptual and theoretical framework for studying the human postural control system is introduced. Mathematical techniques from statistical mechanics are developed and applied to the analysis and interpretation of stabilograms. This work was based on the assumption that the act of maintaining an erect posture could be viewed, in part, as a stochastic process. Twenty-five healthy young subjects were studied under quiet-standing conditions. Center-of-pressure (COP) trajectories were analyzed as one-dimensional and two-dimensional random walks. This novel approach led to the extraction of repeatable, physiologically meaningful parameters from stabilograms. It is shown that although individual stabilograms for a single subject were highly variable and random in appearance, a consistent, subject-specific pattern emerged with the generation of averaged stabilogram-diffusion plots (mean square COP displacement vs time interval). In addition, significant inter-subject differences were found in the calculated results. This suggests that the steady-state behavior of the control mechanisms involved in maintaining erect posture can be quite variable even amongst a population of age-matched, anthropometrically similar, healthy individuals. These posturographic analyses also demonstrated that COP trajectories could be modelled as fractional Brownian motion and that at least two control systems – a short-term mechanism and a long-term mechanism – were operating during quiet standing. More specifically, the present results suggest that over short-term intervals open-loop control schemes are utilized by the postural control system, whereas over long-term intervals closed-loop control mechanisms are called into play. This work strongly supports the position that much can be learned about the functional organization of the postural control system by studying the steady-state behavior of the human body during periods of undisturbed stance.

**Key words:** Postural control – Open-loop control – Closed-loop control – Random walk – Human

Correspondence to: J.J. Collins

## Introduction

The task of maintaining an upright posture involves a complex sensorimotor control system. Even when a young, healthy individual attempts to stand still, the center of gravity of his or her body and the center of pressure (COP) under his or her feet move relative to a global coordinate system. A plot of the time-varying coordinates of the COP is known as a stabilogram (Fig. 1). A number of biomechanical researchers have attempted to evaluate postural sway by using a force platform to measure the anteroposterior and mediolateral displacements of the COP over the plane of support. However, previous attempts at interpreting stabilograms from a motor control perspective have not been successful. Many of the earlier studies limited the analysis of these plots to summary statistics, i.e., calculation of the length of sway path, average radial area, etc. (Diener et al. 1984; Kirby et al. 1987; Norré et al. 1987; Hasan et al. 1990). By doing so, these investigations ignored the dynamic characteristics of stabilograms, i.e., the magnitude and direction of displacements between adjacent points, the temporal ordering of a series of COP coordinates, etc.

The majority of contemporary scientific and clinical investigations in postural control have directed their attention to analyzing the response of the human body to various external perturbations (Moore et al. 1988; Woolacott et al. 1988; Diener et al. 1988, 1991; Horak et al. 1990; Dietz et al. 1991). Although this reflexive approach enables one to examine the input/output characteristics of different closed-loop feedback systems (Nashner 1971, 1972), it does not consider explicitly the stabilizing roles of possible open-loop control schemes or the steady-state behavior of the human body during periods of undisturbed stance. Furthermore, the experimental protocols associated with dynamic posturography are considerably more hazardous and physically taxing than those involved in static posturography. Also, the output of a perturbation or input impulse is modulated by the state of excitation or alertness of the individual (Horak et al. 1989; Beckley et al. 1991). Thus, from a clinical standpoint, static posturogra-

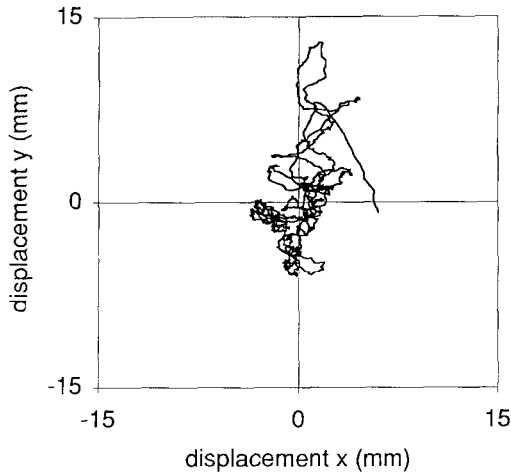


**Fig. 1.** Typical 30-s stabilogram for a healthy young individual during quiet standing. Mediolateral and anteroposterior COP displacements are plotted along the  $x$ -axis and  $y$ -axis, respectively

phy is a much simpler and safer test to perform and administer to aged and disabled individuals. Nonetheless, to date, the utility of static posturography in the clinic and laboratory has been limited by the lack of a reliable, consistently useful approach or technique for extracting repeatable, physiologically meaningful information from stabilograms.

In the present study, the problem of characterizing stabilograms is approached from the perspective of statistical mechanics. In particular, it is postulated that the movement of the center of pressure during quiet standing can be modelled as a system of coupled, correlated random walks, i.e., the motion is considered to be the result of a combination of deterministic and stochastic mechanisms. In order to test this hypothesis, probabilistic tools and techniques from statistical mechanics will be introduced into the experimental domain of posturography. One of the aims of this work is to develop a general stochastic modelling framework to examine and interpret center-of-pressure time series. In this way, it is hoped that the present approach will lead to a greater understanding of the strategies utilized by the postural control system to maintain the complex, multi-degree-of-freedom structure of the musculoskeletal system in equilibrium with external forces during quiet standing.

## Materials and methods

### Application of statistical mechanics

Fundamental concepts and principles from statistical mechanics have been applied to the study of a number of different neurophysiological systems and phenomena (Holden 1976; Tuckwell 1989). Bartol et al. (1991), for instance, utilized diffusion theory and stochastic methods for modelling miniature endplate current generation in neuromuscular junctions. In a classic study, Gerstein and Mandelbrot (1964) represented the statistical properties of spike trains of single neurons as random walks towards an absorbing barrier. Recently, this work has been extended to more detailed

analyses of how information is encoded and transmitted by neurons (Gorse and Taylor 1990; Longtin et al. 1991). Others have used statistical physics models to simulate and analyze the collective dynamics and emergent properties of large networks of coupled neurons (Peretto 1984; Sompolinsky 1988).

The general driving principle of statistical mechanics is that although the outcome of an individual random event is unpredictable, it is still possible to obtain definite expressions for the probabilities of various aspects of a stochastic process or mechanism. A classic example of a statistical mechanical phenomenon is Brownian motion. The simplest case of Brownian motion is the random movement of a single particle along a straight line. This construct is known as a one-dimensional random walk. In 1905, Einstein studied Brownian motion and showed that the mean square displacement  $\langle \Delta x^2 \rangle^1$  of a one-dimensional random walk was related to the time interval  $\Delta t$  by the expression:

$$\langle \Delta x^2 \rangle = 2D\Delta t \quad (1)$$

where the parameter  $D$  is the diffusion coefficient. In words, the diffusion coefficient is an average measure of the stochastic activity of a random walker, i.e., it is directly related to its jump frequency and/or amplitude. The above result is easily extended to higher dimensions, i.e., random walks in a plane or in three-dimensional space. In each case, the mean square displacement and time interval are still linearly related.

The term *fractional Brownian motion* was introduced by Mandelbrot and van Ness (1968) to designate a generalized family of Gaussian stochastic processes. This mathematical concept, which is an extension of classical or ordinary Brownian motion, has been used to model a number of different natural objects and phenomena, including landscape terrains and fluid turbulence (Mandelbrot 1983). Accessible introductions to the subject are provided by Feder (1988), Saupe (1988) and Voss (1988). For the purposes of the present study, it is important to point out that for fractional Brownian motion the Einstein relation given by Eq. 1 is generalized to the following scaling law:

$$\langle \Delta x^2 \rangle \sim \Delta t^{2H} \quad (2)$$

where the scaling exponent  $H$  can be any real number in the range  $0 < H < 1$ . For classical Brownian motion,  $H = \frac{1}{2}$ . As can be seen from Eq. 2, the scaling exponent  $H$  can be determined from the slope of the log-log plot of the mean square displacement versus  $\Delta t$  curve.

An important feature of fractional Brownian motion is that past increments in a particle's displacement are correlated with future increments. The only exception to this rule is the case  $H = \frac{1}{2}$ , which, as stated earlier, corresponds to a classical random walk.<sup>2</sup> For fractional Brownian motion, the correlation function  $C$ , which is time-independent, is given by the expression (Feder 1988):

$$C = 2(2^{2H-1} - 1). \quad (3)$$

Note that for  $H > \frac{1}{2}$ , the stochastic process is positively correlated, i.e.,  $C > 0$ . In this case, a fractional Brownian particle moving in a particular direction for some  $t_0$  will tend to continue in the same direction for  $t > t_0$ . In general, increasing (decreasing) trends in the past imply on the average increasing (decreasing) trends in the future (Feder 1988; Saupe 1988). This type of behavior is known as *persistence*.

The opposite situation occurs for  $H < \frac{1}{2}$  – past and future increments are negatively correlated. Thus, an increasing (decreasing) trend in the past implies a decreasing (increasing) trend in the future. This type of stochastic behavior is referred to as *anti-persistence*.

<sup>1</sup> The angled brackets  $\langle \cdot \rangle$  denote an average over time or an ensemble average over a large number of samples.

<sup>2</sup> The increments in displacement making up ordinary Brownian motion are statistically independent.

Experimental methods

Twenty-five healthy male subjects of similar age (19–27 years, mean 22.3 years) and size (body weight 59.1–85.0 kg, mean 71.8 kg; height 165.1–186.7 cm, mean 174.9 cm) were included in the study. The members of the subject population had no evidence or known history of a gait, postural or skeletal disorder. Informed consent was obtained from each subject prior to participation. Postural stability was evaluated by using a Kistler 9287 multicomponent force platform to measure the time-varying displacements of the COP under a subject’s feet. Each subject was instructed to stand in an upright posture in a standardized stance on the platform. In the standardized stance, the subjects’ feet were abducted 10° and their heels were separated mediolaterally by a distance of 3 cm. During the testing, the subjects stood barefoot with their arms comfortably at their sides and their eyes open and fixed on a point in front of them. Each trial lasted for a period of 30 s and the force platform data were sampled at a frequency of 100 Hz. A series of 30 trials were conducted for each of the first 10 subjects. This large number of tests was required to assess the reliability of the proposed statistical mechanical methodology. Rest periods of 60 s and 5 min were provided between each trial and between each set of 10 trials, respectively. Ten trials were conducted for each of the remaining 15 subjects.

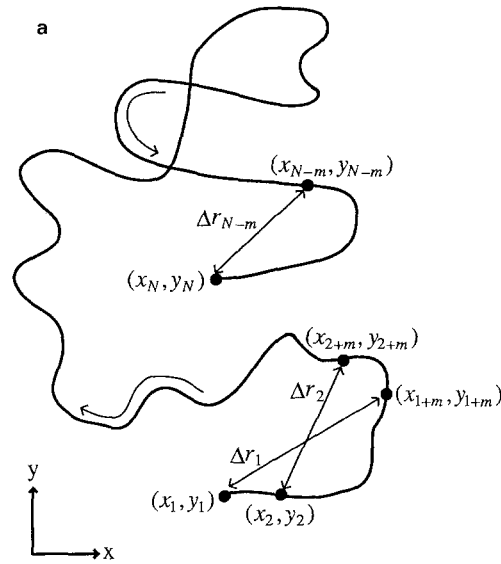
In order to assess the noise characteristics of the Kistler platform, a large mass of approximately 100 kg was placed on the platform. The kinetic data were sampled at 100 Hz for a period of 30 s. In theory, the COP of a static object should be constant as a function of time. It was found, however, that experimental noise introduced variations that were less than ±0.5 mm in magnitude in the measured coordinates of the COP of the test mass.

Data analysis and stabilogram-diffusion plots

The COP trajectories were studied as one-dimensional and two-dimensional random walks. The displacement analysis was carried out by computing the square of the displacements between all pairs of points separated in time by a specified time interval Δt (see Fig. 2a). The square displacements were then averaged over the number of Δt making up the COP time series.<sup>3</sup> This process was repeated for increasing values of Δt. An important point to note is that the number of calculated square displacements was inversely proportional to the size of the time interval. A plot of mean square COP displacement versus time interval Δt will be referred to as a stabilogram-diffusion plot (Fig. 2b).

Experimental studies concerned with diffusion-like processes typically analyze either a long time series of data measurements or a large number of smaller time series of such measurements (Shlesinger and West 1984; Montroll and Lebowitz 1987). In a posturographic investigation, it would be impractical, however, to have subjects stand on a force platform for extended periods of time. Physiological factors such as fatigue would tend to obscure the results. In the present study, it was therefore decided to collect a large number of 30-s trials for each subject and to analyze averaged sets of the results derived from these tests. Specifically, stabilogram-diffusion plots were computed for each subject trial and then 10 such curves were averaged to obtain a resultant stabilogram-diffusion plot for a particular subject. Three resultant plots were thus generated for a subject who participated in 30 trials.

Diffusion coefficients *D* (Eq. 1) were calculated from the slopes of the resultant linear-linear plots of mean square COP displacement versus time interval curves, i.e., <math>\langle \Delta r^2 \rangle</math> vs <math>\Delta t</math>, <math>\langle \Delta x^2 \rangle</math> vs <math>\Delta t</math>, and <math>\langle \Delta y^2 \rangle</math> vs <math>\Delta t</math>. Similarly, scaling exponents *H* (Eq. 2) were computed from the resultant log-log plots of such curves. In all cases, the slopes were determined by utilizing the method of least squares to fit straight



For a given Δt (spanning *m* data intervals):

$$\langle \Delta r^2 \rangle_{\Delta t} = \frac{\sum_{i=1}^{N-m} (\Delta r_i)^2}{(N-m)}$$

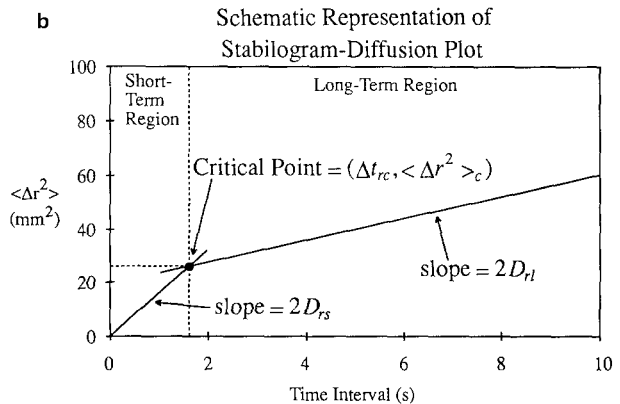


**Fig. 2. a** Diagram showing the method for calculating mean square planar displacement <math>\langle \Delta r^2 \rangle</math> as a function of time interval Δt for a COP trajectory made up of *N* data points  $(x_1, y_1; x_2, y_2; \dots; x_N, y_N)$ . **b.** A typical resultant planar stabilogram-diffusion plot ( $\langle \Delta r^2 \rangle$  vs Δt) generated from COP time series according to the method shown in (a). The diffusion coefficients *D<sub>rs</sub>* and *D<sub>rl</sub>* are computed from the slopes of the lines fitted to the short-term and long-term regions, respectively. The critical point,  $(\Delta t_{rc}, \langle \Delta r^2 \rangle_c)$ , is defined by the intersection of the lines fitted to the two regions of the plot. The scaling exponents *H<sub>rs</sub>* and *H<sub>rl</sub>* are calculated from the slopes of the log-log plots of the short-term and long-term regions, respectively

lines through defined portions of the aforementioned plots. All parameters were determined by a single investigator.

Intraclass correlation coefficients (ICCs) were calculated to determine the degree of agreement between the respective stabilogram-diffusion parameters which were extracted from the three resultant plots for each of the first 10 subjects. The ICC equation for a *random effects* model, i.e., ICC equation (2.1) as described by Shrout and Fleiss (1979), was used in the present study. This equation is given by

<sup>3</sup> In the present study,  $\{x_i\}$  and  $\{y_i\}$  are the mediolateral and anteroposterior COP time series, respectively, and  $\langle \Delta r^2 \rangle = \langle \Delta x^2 \rangle + \langle \Delta y^2 \rangle$ .

the expression:

$$ICC(2, 1) = \frac{BMS - EMS}{BMS + (k - 1) EMS + k(JMS - EMS)/n} \quad (4)$$

where  $n$  is the number of subjects,  $k$  is the number of repeated measures (judges) per subject, and BMS, JMS and EMS are the between-subjects mean square, between-judges mean square and error mean square, respectively. See Shrout and Fleiss (1979) for further details.

Although there are no rigorous, universally accepted standards for assessing reliability, Fleiss (1986) offered the following general guidelines: ICC values less than 0.4 represent poor reliability, ones between 0.4 and 0.75 represent fair to good reliability, and values greater than 0.75 correspond to excellent reliability. This categorization was adopted in this investigation.

## Results

Resultant planar stabilogram-diffusion plots for four representative subjects are shown in Fig. 3. It is important to note that the posturographic results of Fig. 3 were qualitatively different from those expected for ordinary Brownian motion. Whereas the mean square displacement of a random walk grows linearly with a constant slope for increasing time interval [see Eq. 1], the stabilogram-diffusion curves changed slope after a transition or critical point at some small  $\Delta t$ . This general feature was found in the calculated results for all 25 subjects who participated in the present investigation. As will be described below, COP trajectories also differed from classical Brownian motion in other ways.

In order to parameterize the above stabilogram-diffusion plots, two regions were identified – a short-term region and a long-term region. These regions were separated by a transition period where the slope of the stabilogram-diffusion plot changed considerably. Diffusion coefficients and scaling exponents were calculated for each region (Fig. 2b). Subscripts  $s$  and  $l$  will be used throughout the manuscript to denote the short-term and long-term regions, respectively. The lines fitted for computation of  $D_{js}$ ,  $D_{jl}$ ,  $H_{js}$ , and  $H_{jl}$  (where  $j = x, y, r$ ) had  $r^2$  values that ranged from 0.97 to 1.00, 0.65 to 0.99, 0.90 to 1.00, and 0.68 to 1.00, respectively. An estimate for each critical point was determined as the intersection point of the straight lines fitted to the two regions of the linear-linear version of each resultant stabilogram-diffusion plot (Fig. 2b).

### The first group

**Diffusion coefficients.** The means and standard deviations of the calculated diffusion coefficients for the first 10 subjects are given in Table 1. Several general points should be noted. Firstly, in all cases, the short-term diffusion coefficients were much greater than the respective long-term coefficients, i.e.,  $D_{js} \gg D_{jl}$  where  $j = x, y, r$ . Secondly, for the majority of subjects, the anteroposterior diffusion coefficients were greater than their mediolateral counterparts, i.e.,  $D_{yi} > D_{xi}$  where  $i = s, l$ . This result was not unexpected given the fact that anteroposterior postural

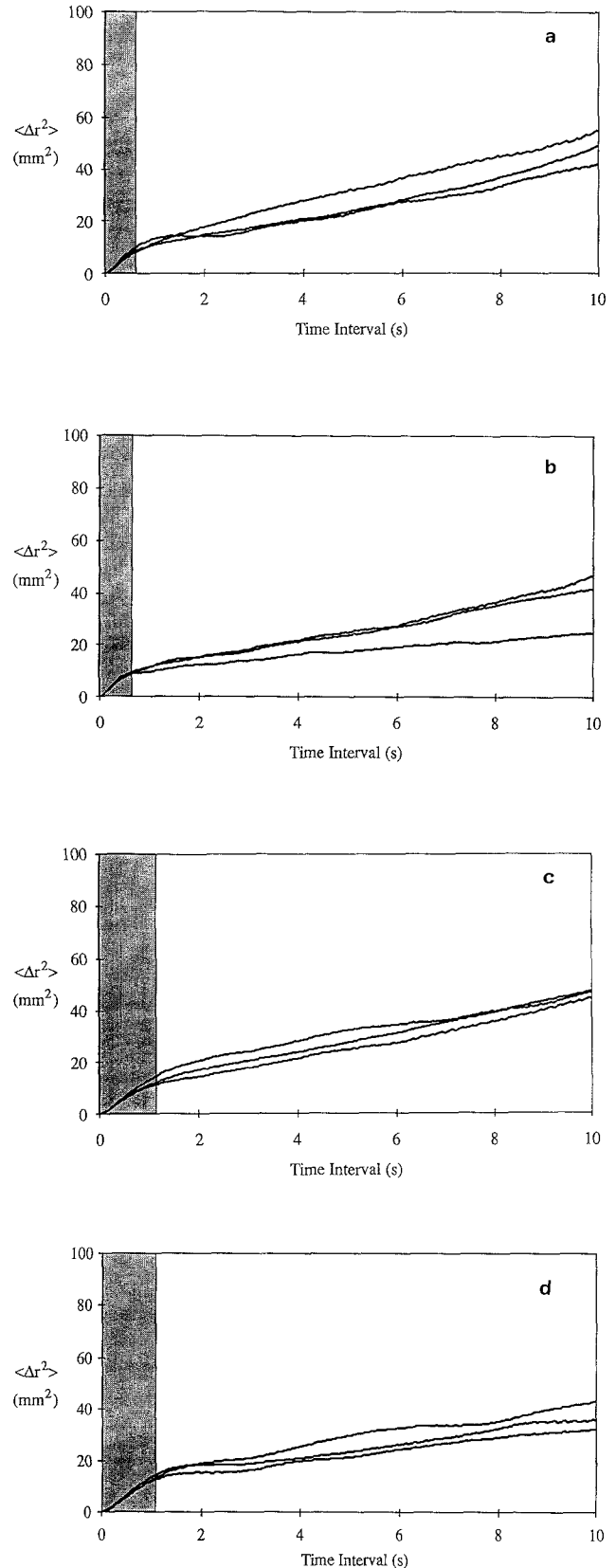


**Fig. 3a–d.** Resultant planar stabilogram-diffusion plots. Each resultant curve is generated from ten different 30-s COP time series. The approximated short-term region in each graph is shaded. **a** Subject 1; **b** subject 3; **c** subject 4; **d** subject 5. The calculated results for these subjects are given in Tables 1–3

**Table 1.** Diffusion coefficients ( $\text{mm}^2 \text{s}^{-1}$ ): means and standard deviations for the first population of subjects ( $n=10$ )

Subject	Mediolateral (x)		Anteroposterior (y)		Planar (r)	
	$D_{xs}$	$D_{xi}$	$D_{ys}$	$D_{yi}$	$D_{rs}$	$D_{ri}$
1	$3.23 \pm 0.52$	$0.60 \pm 0.28$	$5.05 \pm 0.25$	$1.37 \pm 0.07$	$8.28 \pm 0.74$	$1.97 \pm 0.23$
2	$2.33 \pm 0.16$	$0.24 \pm 0.07$	$4.10 \pm 0.62$	$0.55 \pm 0.49$	$6.43 \pm 0.53$	$0.79 \pm 0.45$
3	$3.35 \pm 0.22$	$0.32 \pm 0.14$	$6.10 \pm 0.86$	$1.13 \pm 0.53$	$9.45 \pm 0.67$	$1.45 \pm 0.57$
4	$2.91 \pm 0.54$	$0.64 \pm 0.05$	$4.06 \pm 0.19$	$1.09 \pm 0.25$	$6.97 \pm 0.47$	$1.73 \pm 0.21$
5	$3.47 \pm 0.49$	$0.31 \pm 0.08$	$3.16 \pm 0.58$	$1.02 \pm 0.15$	$6.62 \pm 0.70$	$1.32 \pm 0.13$
6	$4.31 \pm 0.33$	$0.19 \pm 0.14$	$7.26 \pm 1.84$	$1.00 \pm 0.30$	$11.57 \pm 2.06$	$1.19 \pm 0.33$
7	$2.89 \pm 0.44$	$0.96 \pm 0.63$	$2.72 \pm 0.29$	$1.11 \pm 0.12$	$5.60 \pm 0.73$	$2.06 \pm 0.57$
8	$1.20 \pm 0.23$	$0.21 \pm 0.14$	$2.46 \pm 0.41$	$0.45 \pm 0.11$	$3.66 \pm 0.32$	$0.66 \pm 0.03$
9	$2.53 \pm 0.21$	$0.80 \pm 0.38$	$4.08 \pm 0.53$	$1.47 \pm 0.38$	$6.61 \pm 0.65$	$2.27 \pm 0.29$
10	$0.58 \pm 0.16$	$0.13 \pm 0.04$	$1.63 \pm 0.11$	$1.06 \pm 0.25$	$2.21 \pm 0.26$	$1.19 \pm 0.22$
GM $\pm$ SD	$2.68 \pm 1.10$	$0.44 \pm 0.35$	$4.06 \pm 1.76$	$1.02 \pm 0.40$	$6.74 \pm 2.68$	$1.46 \pm 0.59$

Group means (GM) and standard deviations (SD) for the respective parameters are given in the last row

sway is typically greater than mediolateral sway. Thirdly, since

$$\langle \Delta r^2 \rangle = \langle \Delta x^2 \rangle + \langle \Delta y^2 \rangle \quad (5)$$

it follows that the respective planar diffusion coefficients are linear combinations of the diffusion coefficients calculated for the  $x$  and  $y$  directions, i.e.,  $D_{ri} = D_{xi} + D_{yi}$ .

It should also be pointed out that two subjects, subjects 8 and 10, exhibited relatively small diffusion coefficients  $D_{ji}$  (Table 1). Similarly, very small (close to zero) long-term mediolateral diffusion coefficients were calculated for subject 6. In the case of subject 6, his COP had fully explored the characteristic space for mediolateral sway during the early stages of the long-term region of the stabilogram-diffusion plot. In other words, after some small  $\Delta t$ , the COP no longer moved farther away along the  $x$ -axis, on average, from some relative central point. Under these conditions, the COP trajectory is said to have saturated to some boundary value. Since the COP is limited to the area of support defined by a subject's feet, it is expected that a stabilogram would also saturate to a systematic boundary value in the anteroposterior direction. However, for the maximum time interval considered in the present stabilogram-diffusion plots (Fig. 3), i.e.,  $\Delta t_{max} = 10$  s, such an effect was not found for any of the subjects. Longer COP time series are needed to study this phenomenon.<sup>4</sup>

**Scaling exponents.** The means and standard deviations of the computed stabilogram-diffusion scaling exponents for the first 10 subjects are presented in Table 2. For the short-term region, the scaling exponents  $H_{js}$  were, in general, much greater than 0.5. Thus, over short-term intervals during quiet standing, COP trajectories exhibit persistent behavior. On the other hand, long-term scaling exponents  $H_{ji}$  were in nine out of ten cases much less than 0.5 (Table 2). Thus, over long-term intervals, stabilograms exhibit anti-persistence. The only exception to the above

statement was subject 10 who displayed mean values of 0.53 and 0.47 for  $H_{yi}$  and  $H_{ri}$ , respectively. Subject 10's short-term behavior was also different from the other subjects; for example, his mediolateral scaling exponent was close to that expected for an uncorrelated random walk, i.e.,  $H_{xs} \sim 0.5$ . Finally, it should be noted that the long-term mediolateral scaling exponent  $H_{xi}$  for subject 6 was nearly zero (Table 2). This implied that subject 6's mean square COP displacement in the  $x$  direction was essentially constant for increasing values of  $\Delta t$ . This result is a direct consequence of the fact that the COP trajectories for subject 6 saturated to a mediolateral boundary value during the early stages of the long-term region (as noted above).

**Critical point coordinates.** The estimated values of the time intervals and mean square displacements defining the stabilogram-diffusion critical points for the first 10 subjects are presented in Table 3. In general, the transition points occurred at relatively small time intervals, i.e.,  $\Delta t_{jc}$  ranged from 0.33 to 1.67 s with a mean of approximately 1.0 s. On the other hand, the critical mean square displacements ranged from very small values, i.e.,  $1.10 \text{ mm}^2$  for  $\langle \Delta x^2 \rangle_c$ , to rather large ones, i.e.,  $29.37 \text{ mm}^2$  for  $\langle \Delta r^2 \rangle_c$ . It is important to point out that the critical points were ill-defined for many of the subjects. In these cases, the slope of a stabilogram-diffusion plot did not change abruptly at a distinct point, but rather it changed more gradually over a brief time period. Consequently, the numbers given in Table 3 should only be looked upon as rough estimates.

**Reliability.** The intraclass correlation coefficients for the diffusion coefficients, scaling exponents and critical point coordinates for the first 10 subjects are given in Table 4. The short-term diffusion coefficients  $D_{js}$  and scaling exponents  $H_{js}$  were highly reliable – ICC values ranged from 0.76 to 0.92. The reliability measures for the long-term scaling exponents  $H_{ji}$  were lower but, in general, good to excellent (Fleiss 1986): ICC values ranged from 0.59 to 0.83. The ICC values for the long-term diffusion coefficients  $D_{ji}$  were lower than those for the short-term diffusion coefficients, i.e., 0.46–0.68 vs 0.83–0.90. In all cases, the reliability measures for the long-term stabilo-

<sup>4</sup> In a preliminary posturographic study using 60-s time series, it was found that several subjects saturated to a characteristic boundary value in the anteroposterior direction after some relatively long time interval, i.e.,  $\Delta t = 30$  s.

**Table 2.** Scaling exponents: means and standard deviations for the first population of subjects ( $n=10$ )

Subject	Mediolateral (x)		Anteroposterior (y)		Planar (r)	
	$H_{xs}$	$H_{xl}$	$H_{ys}$	$H_{yl}$	$H_{rs}$	$H_{rl}$
1	0.71 ± 0.02	0.26 ± 0.05	0.73 ± 0.01	0.39 ± 0.05	0.72 ± 0.01	0.35 ± 0.03
2	0.74 ± 0.02	0.18 ± 0.02	0.81 ± 0.03	0.17 ± 0.10	0.78 ± 0.03	0.17 ± 0.07
3	0.76 ± 0.01	0.18 ± 0.02	0.78 ± 0.02	0.34 ± 0.08	0.77 ± 0.01	0.28 ± 0.06
4	0.78 ± 0.03	0.31 ± 0.05	0.79 ± 0.01	0.30 ± 0.07	0.79 ± 0.02	0.31 ± 0.06
5	0.78 ± 0.01	0.11 ± 0.05	0.76 ± 0.03	0.31 ± 0.01	0.77 ± 0.01	0.24 ± 0.02
6	0.79 ± 0.01	0.06 ± 0.04	0.85 ± 0.02	0.17 ± 0.04	0.82 ± 0.02	0.14 ± 0.03
7	0.77 ± 0.01	0.27 ± 0.10	0.79 ± 0.01	0.34 ± 0.02	0.78 ± 0.01	0.31 ± 0.04
8	0.65 ± 0.02	0.21 ± 0.11	0.71 ± 0.03	0.24 ± 0.05	0.69 ± 0.02	0.23 ± 0.01
9	0.73 ± 0.03	0.29 ± 0.07	0.79 ± 0.03	0.37 ± 0.08	0.76 ± 0.03	0.34 ± 0.03
10	0.57 ± 0.03	0.26 ± 0.05	0.72 ± 0.02	0.53 ± 0.05	0.68 ± 0.01	0.47 ± 0.04
GM ± SD	0.73 ± 0.07	0.21 ± 0.10	0.77 ± 0.05	0.31 ± 0.12	0.76 ± 0.05	0.28 ± 0.10

Group means (GM) and standard deviations (SD) for the respective parameters are given in the last row

**Table 3.** Critical point coordinates [time intervals (s) and mean square displacements ( $\text{mm}^2$ )]: means and standard deviations for the first population of subjects ( $n=10$ )

Subject	Mediolateral (x)		Anteroposterior (y)		Planar (r)	
	$\Delta t_{xc}$	$\langle \Delta x^2 \rangle_c$	$\Delta t_{yc}$	$\langle \Delta y^2 \rangle_c$	$\Delta t_{rc}$	$\langle \Delta r^2 \rangle_c$
1	0.88 ± 0.27	5.38 ± 1.01	0.42 ± 0.32	3.67 ± 2.93	0.61 ± 0.28	9.26 ± 3.57
2	1.20 ± 0.16	5.28 ± 0.40	1.67 ± 0.15	12.85 ± 1.99	1.50 ± 0.10	18.15 ± 2.25
3	0.87 ± 0.17	5.44 ± 1.49	0.33 ± 0.15	3.55 ± 2.14	0.55 ± 0.08	9.34 ± 1.22
4	0.81 ± 0.14	4.15 ± 1.02	1.28 ± 0.67	9.68 ± 5.02	1.06 ± 0.33	13.80 ± 5.40
5	0.83 ± 0.08	5.32 ± 1.02	1.57 ± 0.54	9.57 ± 4.21	1.15 ± 0.27	14.28 ± 3.14
6	1.30 ± 0.16	10.48 ± 2.15	1.36 ± 0.19	18.86 ± 3.37	1.33 ± 0.05	29.37 ± 5.04
7	1.25 ± 0.36	7.15 ± 1.62	1.21 ± 0.54	6.68 ± 2.37	1.23 ± 0.40	13.90 ± 3.45
8	1.23 ± 0.31	2.84 ± 1.24	1.35 ± 0.21	6.51 ± 2.03	1.35 ± 0.10	9.46 ± 1.53
9	1.10 ± 0.68	5.65 ± 3.24	1.00 ± 0.25	7.22 ± 0.97	0.85 ± 0.26	11.03 ± 3.76
10	1.04 ± 0.39	1.10 ± 0.26	0.56 ± 0.18	1.58 ± 0.39	0.72 ± 0.23	2.80 ± 0.64
GM ± SD	1.05 ± 0.32	5.28 ± 2.73	1.07 ± 0.55	8.02 ± 5.44	1.04 ± 0.38	13.14 ± 7.34

Group means (GM) and standard deviations (SD) for the respective parameters are given in the last row

**Table 4.** Intraclass correlation coefficients: ICC (2, 1) for the repeated measures of the stabilogram-diffusion parameters for the first 10 subjects

Diffusion coefficients					
$D_{xs}$	$D_{xl}$	$D_{ys}$	$D_{yl}$	$D_{rs}$	$D_{rl}$
0.90	0.46	0.83	0.46	0.90	0.68
Scaling exponents					
$H_{xs}$	$H_{xl}$	$H_{ys}$	$H_{yl}$	$H_{rs}$	$H_{rl}$
0.92	0.59	0.76	0.73	0.86	0.83
Critical point coordinates					
$\Delta t_{xc}$	$\langle \Delta x^2 \rangle_c$	$\Delta t_{yc}$	$\langle \Delta y^2 \rangle_c$	$\Delta t_{rc}$	$\langle \Delta r^2 \rangle_c$
0.04	0.68	0.58	0.73	0.62	0.80

gram-diffusion parameters were thus lower than those for their short-term counterparts. This result was due largely to the fact that the number of mean square displacements for a particular COP time series was inversely proportional to the size of the time interval  $\Delta t$ . In general, the variability of a statistic describing a stochastic process decreases as the number of measurements made on the system under study is increased. Therefore, it is expected that the computed ICC values for the long-term posturographic parameters would increase as the number of COP time series making up the resultant stabilogram-diffusion plots was increased.

In addition, it should be noted that the reliability measures for the critical point coordinates were highly variable: ICC values for the critical time intervals ranged from 0.04 (poor) to 0.62 (good) whereas those for the critical mean square displacements ranged from 0.68 (good) to 0.80 (excellent). This result can be attributed in part to the inherent limitations of the present method for calculating the transition point coordinates. As described earlier, the position of a critical point was estimated as the point of intersection of the best-fit straight lines that were determined for the two regions of a stabilogram-diffusion plot. Consequently, the variability of both the short-term and long-term diffusion coefficients, which could be combined in either additive or subtractive ways, directly influenced the calculated values and associated variability of the critical point coordinates.

#### The second group

The ranges, group means and standard deviations for the diffusion coefficients, scaling exponents and critical point coordinates for the second subject population ( $n=15$ ) are listed in Table 5. The general qualitative features described for the posturographic results of Tables 1–3 are also appropriate for those presented in Table 5. It is important to note, however, that one of the 15 subjects had a long-

**Table 5.** Ranges, group means and standard deviations (SD) for the diffusion coefficients, scaling exponents, and critical point coordinates for the second population of 15 subjects

Parameter		Range	Group Mean $\pm$ SD
Diffusion coefficients ( $\text{mm}^2 \text{s}^{-1}$ )	$D_{xs}$	1.05–12.44	$3.94 \pm 2.81$
	$D_{xi}$	0.17–2.09	$0.54 \pm 0.47$
	$D_{ys}$	2.57–16.03	$7.27 \pm 4.11$
	$D_{yi}$	0.43–6.73	$2.51 \pm 1.76$
	$D_{rs}$	3.62–26.03	$11.21 \pm 6.43$
	$D_{ri}$	0.60–7.51	$3.05 \pm 2.06$
Scaling exponents	$H_{xs}$	0.63–0.81	$0.74 \pm 0.05$
	$H_{xi}$	0.12–0.32	$0.23 \pm 0.05$
	$H_{ys}$	0.70–0.83	$0.77 \pm 0.04$
	$H_{yi}$	0.18–0.50	$0.38 \pm 0.10$
	$H_{rs}$	0.70–0.82	$0.76 \pm 0.04$
	$H_{ri}$	0.18–0.45	$0.34 \pm 0.08$
Critical point coordinates (s)	$\Delta t_{xc}$	0.63–1.85	$1.06 \pm 0.42$
	$\Delta t_{yc}$	0.35–1.85	$0.97 \pm 0.46$
	$\Delta t_{rc}$	0.44–1.30	$0.92 \pm 0.29$
	$\langle \Delta x^2 \rangle_c$	1.88–20.70	$7.75 \pm 5.74$
Critical point coordinates ( $\text{mm}^2$ )	$\langle \Delta y^2 \rangle_c$	3.87–47.63	$12.69 \pm 10.71$
	$\langle \Delta r^2 \rangle_c$	5.50–64.64	$19.65 \pm 15.72$

term anteroposterior scaling exponent ( $H_{yi}$ ) equal to 0.5. As mentioned earlier, this is the result expected for a classical, i.e., uncorrelated, random walk.

Quantitatively, the group means for the diffusion coefficients  $D_{ji}$  given in Table 5 were, in all cases, larger than those listed in Table 1. This was due mainly to the fact that a small number of the subjects in the second population had very large diffusion coefficients. On the other hand, the group means for the scaling exponents and critical time intervals for the second experimental population (Table 5) were in close agreement with those for the first population (Tables 2 and 3, respectively). However, the respective group means for the critical mean square displacements given in Table 5 were larger, in all cases, than those calculated for the first 10 subjects (Table 3). These displacement differences were a direct consequence of the fact that the critical time intervals for the two groups were equivalent but the average short-term diffusion coefficients for the second subject population were larger than those for the first.

#### Mathematical model development

In this study, it was shown that posturographic time series were qualitatively different from those predicted for ordinary Brownian motion. As described earlier, the diffusion curves for a classical random walk grow linearly and unbounded with increasing time interval whereas stabilogram-diffusion curves change slope after a transition point at some small  $\Delta t$  and then saturate to a relatively constant mean square displacement after some large time interval. Furthermore, whereas the scaling exponent for an uncorrelated random walk should be equal to 0.5, it was demonstrated that the scaling exponents for COP trajectories are greater than and less than 0.5 (persistence/anti-persistence) for short-term and long-term intervals, respectively.

To account for these experimental observations and offer a possible physiological explanation, the movements of the COP during undisturbed stance can be modelled as a system of coupled, bounded random walks. The presumed form of the model was motivated by the calculated dynamic differences between the short-term and long-term regions of the stabilogram-diffusion plots and by the following mechanical/physiological considerations: (1) the erect human body can, in theory, assume an infinite number of different geometric configurations and remain in equilibrium with external forces; (2) since skeletal muscle is incapable of producing purely constant forces (De Luca et al. 1982), body segments acted upon by active muscles are incapable of maintaining purely constant positions and/or orientations. The preliminary mathematical model is composed of two stochastic systems (Fig. 4). The first system consists of a random walker which is attached to a nonlinear spring at the center of a bounded circular area. If the random walker moves away from the center of the circle (its equilibrium point), it is acted upon by a nonlinear, elastic restorative force. The second system, which is linearly superimposed onto the first, consists of another random walker which is bounded by a smaller circular area. In the smaller circle, the walker is acted upon by a system of threshold-based alternating springs, which are attached around the boundary. Once the random walker reaches the perimeter of its bounded area, the spring acting upon the walker is deactivated and the one located on the opposite side of the bounded area is called into play. Thus, for this configuration, the center of the bounded area is *not* a stable equilibrium point. In summary, the COP random walker for each modelled system is perturbed at any given time by both a randomly fluctuating force and a stabilizing and/or destabilizing spring force.

The behavior of the above posturographic model can be described by a simple set of equations. For example, the dynamics of the first COP random walker (which moves

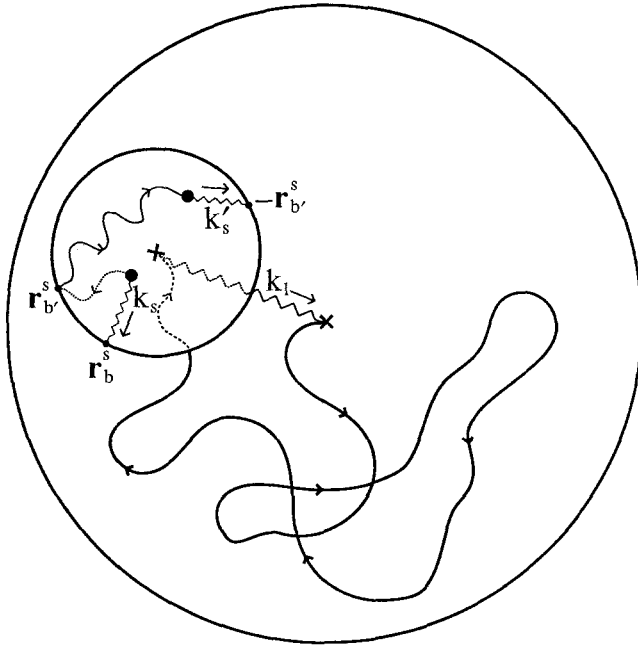


**Fig. 4.** Diagram of the model system of coupled, bounded random walks. The first system consists of a COP random walker which is acted upon by a spring (with stiffness  $k_l$ ) which is attached to the center of the larger circular area. Linearly superimposed onto this random walker is another bounded system. In the smaller bounded area, a second COP random walker is acted upon by a system of threshold-based alternating springs. In the diagram, the random walker is initially acted upon by a spring (with stiffness  $k_s$ ) attached at  $\mathbf{r}_b^s$ . After the random walker crosses the boundary at  $\mathbf{r}_b^s$ , the first spring is turned off and the spring (with stiffness  $k_s'$ ) attached at  $-\mathbf{r}_b^s$  is activated

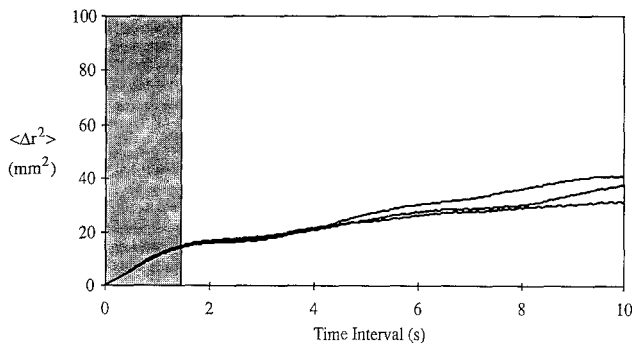


**Fig. 5.** Resultant planar stabilogram-diffusion plots generated by the posturographic model of Fig. 4. Each resultant curve is generated from ten different 30-s simulated COP time series. The approximated short-term region for the system is shaded

within the larger bounded area) is governed by the expression:<sup>5</sup>

$$\mathbf{r}_{n+1}^l = \mathbf{r}_n^l + \xi_n^l + \mathbf{F}^l(\mathbf{r}_{org}^l - \mathbf{r}_n^l) \quad (6)$$

where  $\mathbf{r}_{n+1}^l$  and  $\mathbf{r}_n^l$  are the positions of the random walker at times  $t=n+1$  and  $t=n$ , respectively,  $\xi_n^l$  represents the influence of a randomly fluctuating force, and  $\mathbf{F}^l(\mathbf{r}^l)$  repre-

<sup>5</sup> The origin of each local coordinate system is located at the center of its bounded area.

sents the influence of a restorative spring located at the center ( $\mathbf{r}_{org}^l$ ) of the bounded area. The behavior of the second COP random walker (which moves within the smaller bounded area) is governed by the following equations:

$$\mathbf{r}_{n+1}^s = \mathbf{r}_n^s + \xi_n^s + \mathbf{F}^s(\mathbf{r}_b^s - \mathbf{r}_n^s) \quad \text{if } |\mathbf{r}_n^s| < |\mathbf{r}_b^s| \quad (7)$$

$$\mathbf{r}_{n+1}^s = \mathbf{r}_n^s + \xi_n^s + \mathbf{F}^s(-\mathbf{r}_{b'}^s - \mathbf{r}_n^s) \quad \text{if } |\mathbf{r}_n^s| \geq |\mathbf{r}_b^s| \quad (8)$$

where the above terms are equivalent to those in Eq. 6 except that  $\mathbf{F}^s(\mathbf{r}^s)$  in Eq. 7 represents the influence of a perimeter-based spring attached at point  $\mathbf{r}_b^s$ . If the second COP random walker crosses the boundary at  $\mathbf{r}_b^s$ , then the first spring acting in Eq. 7 is turned off and a spring attached at point  $-\mathbf{r}_{b'}^s$  is activated, as shown in Eq. 8 and Fig. 4.

The above equations formed the basis of an initial-phase computer program. In order to compare the simulation results with experimental data, the computer model was used to generate different sets of 10 time series of 3000 data pairs. Resultant stabilogram-diffusion curves were then calculated according to the methods described earlier. Representative results of the model are shown in Fig. 5. The simulation curves of Fig. 5 are remarkably similar in shape and form to the experimental plots of Fig. 3. For example, it is clear that the simulated diffusion curves changed slope after some small time interval, i.e.,  $\Delta t \sim 1.0$  s. Moreover, over short-term and long-term intervals, the stabilogram model exhibited persistent (simulated  $H_{js} > 0.5$ ) and anti-persistent (simulated  $H_{jl} < 0.5$ ) behavior, respectively. Finally, an important feature of the present computer model was that the qualitative and quantitative characteristics of the simulated stabilogram-diffusion curves could be modified by varying the magnitude of the different parameters that defined the model's behavior.

## Discussion

### Reliability

Before any new technique can be usefully employed as a scientific and/or clinical tool, its reliability must be assessed. In this study, intraclass correlation coefficients were calculated to determine the degree of agreement between repeated measures of the respective stabilogram-diffusion parameters – diffusion coefficients, scaling exponents, and critical point coordinates. It was shown that the majority of the proposed posturographic parameters demonstrated good to excellent reliability. The key analytical advancement of the present work was the utilization of trial averaging. Due to the stochastic nature of stabilograms, it is difficult, conceptually and practically, to obtain repeatable parameters from individual 30-s COP time series. As evidenced by the reported results, this task is greatly simplified by looking at ensemble averages of a relatively small number of experimental sequences, i.e., ten 30-s tests. As mentioned earlier, it is expected that the reliability of the respective parameters would improve as the number of COP time series making up the resultant stabilogram-

diffusion plots was increased. However, because of the complications associated with subject fatigue, any clinical or scientific investigation in posturography will have to accept some trade-off between reliability and experimental practicality.

#### *Open-loop and closed-loop control strategies*

By analyzing stabilograms as fractional Brownian motion, it was revealed that at least two distinctly different neuromuscular control mechanisms – one which exhibits persistence and another which exhibits anti-persistence – are functioning during quiet standing. More specifically, these analyses suggest that over short-term intervals open-loop control schemes are utilized by the postural control system, whereas over long-term intervals closed-loop control mechanisms are called into play. These issues will be discussed in greater detail in the following sections.

#### *Physiologically meaningful posturographic parameters*

Posturography has been limited by the lack of an analytical technique for extracting physiologically meaningful parameters from stabilograms. Since the COP is a measure of whole-body dynamics, it represents the summed effect of a number of different neuromusculoskeletal components acting at a number of different joints. This inherent feature has confounded the majority of previous attempts at interpreting stabilograms from a motor control perspective. An advantage of the proposed stabilogram-diffusion parameters is that they can be directly related to the resultant steady-state behavior and functional interaction of the open-loop and closed-loop neuromuscular mechanisms underlying postural control.

Diffusion coefficients, for example, reflect the level of stochastic activity of the COP along the mediolateral or anteroposterior axis or about the plane of support. These measures can thus be used to quantify postural instability, i.e., larger  $D_{ji}$  correspond to a less tightly regulated or “more random” control system and vice versa.<sup>6</sup> In light of these comments, several aspects of the calculated results should be discussed. Firstly, it was found that the short-term diffusion coefficients were much larger than the long-term coefficients. This suggests that the open-loop control mechanisms which dominate short-term intervals have a higher level of stochastic activity than the closed-loop control mechanisms which are utilized over long-term intervals. Secondly, it was shown that the anteroposterior

diffusion coefficients were greater than the respective mediolateral coefficients. This asymmetry can be attributed largely to the geometry of the lower limb. The ankle or tibiotarsal joint is, for example, mainly a simple hinge joint which allows rotation (plantarflexion/dorsiflexion) in the sagittal plane. Thus, from a passive mechanical standpoint, upright bipedal stance is considerably more stable in the frontal plane than in the sagittal plane. Thirdly, it can be seen in Tables 1 and 5 that the magnitudes of the diffusion coefficients were highly variable amongst young healthy subjects. For instance, there was an order of magnitude difference in the calculated value of the long-term planar diffusion coefficient  $D_{r1}$  for subject 10 (Table 1) and one of the subjects of the second population (Table 5): 1.19 vs 26.03 mm<sup>2</sup> s<sup>-1</sup>. This implies that subject 10 was more stable than the other individual. On a larger scale, these differences suggest that the steady-state behavior of the control mechanisms involved in maintaining erect posture can be quite variable even amongst a population of age-matched, anthropometrically similar, healthy individuals.

The second set of stabilogram-diffusion parameters were the scaling exponents, which quantify the correlation between the step increments making up an experimental stabilogram time series. For the short-term region, the computed scaling exponents were much greater than 0.5. Thus, over short-term intervals during quiet standing, the COP behaved as a positively correlated random walk, i.e., one which tends to move away from some relative equilibrium point following an external perturbation (indicative of open-loop control). On the other hand, it was found that the scaling exponents were much less than 0.5 for the long-term region. Thus, over long-term intervals, the COP behaved as a negatively correlated random walk, i.e., one which tends to return to a relative equilibrium point following a perturbation (indicative of closed-loop control). These results imply that for the majority of subjects the movements of the COP during undisturbed stance are not purely random,<sup>7</sup> i.e.,  $H_{ji} \neq 0.5$ . Instead, these motions most likely represent the combined output of co-existent deterministic and stochastic mechanisms.<sup>8</sup> Finally, it should be noted that the scaling exponent inter-subject variability (Tables 2 and 5) was less than that for the diffusion coefficients (Tables 1 and 5): the coefficients of variation for the scaling exponents were, in general, smaller than those for the diffusion coefficients. Thus, this functional aspect of the postural control system, i.e., the stabilizing/destabilizing effects of different control mech-

<sup>6</sup> It is important to point out, however, that an individual may have relatively large diffusion coefficients  $D_{ji}$  and relatively small critical mean square displacements and/or saturation points. In this case, the postural control system allows a relatively high level of stochastic activity within a relatively small region of the base of support. It should also be noted that it is possible for two individuals to have similar scaling exponents but significantly different diffusion coefficients. For this situation, the COP step increments for the two subjects are similarly correlated, but the average mean square displacement (over a given time interval) is larger for one subject as compared to the other.

<sup>7</sup> A small number of the subjects had scaling exponents which were approximately equal to 0.5, i.e., the result expected for classical Brownian motion.

<sup>8</sup> It is important to emphasize the fact that the COP displacements measured in the present study were principally associated with postural sway and not instrumentation noise – the maximum fluctuations introduced by instrumentation noise were less than 5% of the maximum displacement of the COP during a typical 30-s trial (see Materials and methods). The presence of low levels of electronic/instrumentation noise would, however, decrease the correlation between the COP step increments and thereby shift the values of the respective scaling exponents closer to 0.5.

anisms, may be more consistent within a particular subject population.

The third set of posturographic parameters were the critical point coordinates – the critical time intervals and critical mean square displacements. From an analytical standpoint, these coordinates approximate the transition point at which the slope of a resultant stabilogram-diffusion plot changes considerably. From a physiological standpoint, these coordinates represent the point at which the postural control system switches over from open-loop control to closed-loop control. On average, this crossover point occurred at relatively small time intervals, i.e.,  $\Delta t_{jc} \sim 1.0$  s, and mean square displacements, i.e.  $\langle \Delta j^2 \rangle_c$  was less than  $20.0 \text{ mm}^2$ . A related parameter which was not fully explored in the present investigation was the *saturation point*. This point, which is a function of mean square displacement and time interval, corresponds to a systematic boundary value for large-scale COP movement and the characteristic time it takes the COP to *saturate* to that value. Beyond the saturation point, the diffusion coefficients and scaling exponents should approximate zero. The saturation point can thus be viewed as an average measure of the operational “safety limits” allowed by an individual’s postural control system during quiet standing. It was observed that several subjects saturated to a boundary value in the mediolateral direction in  $\Delta t < 10$  s. A similar anteroposterior effect was not seen in any of the subjects. This posturographic phenomenon – anteroposterior postural sway saturation – requires longer COP time series and correspondingly larger  $\Delta t_{max}$ .

### Physiological interpretations

During any given task, the human postural control system receives information from the visual, vestibular and somatosensory systems. In the past, it was generally believed that these afferent signals were utilized to regulate and continually modify the activity of the musculature during quiet standing. The present posturographic results, however, do not support this view. Instead, these analyses indicate that in addition to the above closed-loop feedback mechanisms, the postural control system also employs open-loop control schemes, the output of which may take the form of descending commands to different postural muscles. Since skeletal muscles are incapable of producing purely constant forces (De Luca et al. 1982), these open-loop activation signals result in small mechanical fluctuations at various joints of the body. The present work suggests that these fluctuations and their associated drift effects are left unchecked by the postural control system until they exceed some systematic threshold, after which corrective feedback mechanisms are called into play. As noted above, the stabilogram-diffusion critical point coordinates quantify the spatial and temporal characteristics of this switching phenomenon. It is important to point out that within this conceptual model, the central nervous system still continually receives afferent information from peripheral sensory organs; however, such information is not used to modulate the efferent signals transmitted to postural muscles unless a certain threshold value is ex-

ceeded. This open-loop/closed-loop control strategy, which allows a certain amount of “sloppiness” in balance control, may have evolved to take account of the inherent time delays of feedback loops and to simplify the task of integrating vast amounts of sensory information when the system is not in jeopardy of instability.

There are a number of possible sources which may set the coordinates of the stabilogram-diffusion critical point. Firstly, for example, its position may be determined by a proprioceptive “dead zone”, i.e., a region over which slight variations in body segment position and orientation are left unchanged. Within this scenario, the critical mean square displacement quantifies an individual’s first-level stability limit, i.e., a primary feedback threshold. An alternative way one could get a “dead zone” would be through the interaction of postural responses with the body’s inertia. Postural responses have time delays of  $\sim 100$  ms (Nashner 1977), whereas the musculoskeletal system has rigid-body time constants which may be on the order of  $\sim 1$  s. The system inertia may thus cause a temporal “dead zone” for response during which the central nervous system is in an open-loop control mode. Another possibility is that the position of the transition point is related to the destabilizing influence of gravity. If this were the case, it would be expected that the critical point coordinates would change in a reduced-gravity environment. Finally, the stabilogram-diffusion critical point may be established by fixed, pre-programmed central commands that are utilized in quiet stance. Central programs for postural control have previously been discussed in the context of perturbation experiments (Horak and Nashner 1986; Dietz 1992).

*Acknowledgements.* This study was supported by the Rehabilitation and Development Service of Veterans Affairs and Liberty Mutual Insurance Company. The authors would like to thank Professor Guido Sandri for many helpful discussions and Michael Rosenstein for his assistance with software development and the preparation of figures.

### References

- Bartol TM, Land BR, Salpeter EE, Salpeter MM (1991) Monte Carlo simulation of miniature endplate current generation in the vertebrate neuromuscular junction. *Biophys J* 59: 1290–1307
- Beckley DJ, Bloem BR, Remler MP, Roos RAC, Van Dijk JG (1991) Long latency postural responses are functionally modified by cognitive set. *Electroencephalogr Clin Neurophysiol* 81: 353–358
- De Luca CJ, LeFever RS, McCue MP, Xenakis AP (1982) Control scheme governing concurrently active human motor units during voluntary contractions. *J Physiol (Lond)* 329: 129–142
- Diener HC, Dichgans J, Bacher M, Gompf B (1984) Quantification of postural sway in normals and patients with cerebellar diseases. *Electroencephalogr Clin Neurophysiol* 57: 134–142
- Diener HC, Horak FB, Nashner LM (1988) Influence of stimulus parameters on human postural responses. *J Neurophysiol* 59: 1888–1905
- Diener HC, Horak F, Stelmach G, Guschlbauer B, Dichgans J (1991) Direction and amplitude precuing has no effect on automatic posture responses. *Exp Brain Res* 84: 219–223
- Dietz V (1992) Human neuronal control of automatic functional movements: interaction between central programs and afferent input. *Physiol Rev* 72: 33–69

- Dietz V, Trippel M, Discher M, Horstmann GA (1991) Compensation of human stance perturbations: selection of the appropriate electromyographic pattern. *Neurosci Lett* 126: 71–74
- Einstein A (1905) Über die von der molekularkinetischen Theorie der Wärme geforderte Bewegung von in ruhenden Flüssigkeiten suspendierten Teilchen. *Ann Phys* 322: 549–560
- Feder J (1988) *Fractals*. Plenum Press, New York
- Fleiss JL (1986) *The design and analysis of clinical experiments*. Wiley, New York
- Gerstein GL, Mandelbrot B (1964) Random walk models for the spike activity of a single neuron. *Biophys J* 4: 41–68
- Gorse D, Taylor JG (1990) A general model of stochastic neural processing. *Biol Cybern* 63: 299–306
- Hasan SS, Lichtenstein MJ, Shiavi RG (1990) Effect of loss of balance on biomechanics platform measures of sway: influence of stance and a method for adjustment. *J Biomech* 23: 783–789
- Holden AV (1976) *Models of the stochastic activity of neurones*. Springer-Verlag, Berlin Heidelberg New York
- Horak FB, Diener HC, Nashner LM (1989) Influence of central set on human postural responses. *J Neurophysiol* 62: 841–853
- Horak FB, Nashner LM (1986) Central programming of postural movements: adaptation to altered support-surface configurations. *J Neurophysiol* 55: 1369–1381
- Horak FB, Nashner LM, Diener HC (1990) Postural strategies associated with somatosensory and vestibular loss. *Exp Brain Res* 82: 167–177
- Kirby RL, Price NA, MacLeod DA (1987) The influence of foot position on standing balance. *J Biomech* 20: 423–427
- Longtin A, Bulsara A, Moss F (1991) Time-interval sequences in bistable systems and the noise-induced transmission of information by sensory neurons. *Phys Rev Lett* 67: 656–659
- Mandelbrot BB (1983) *The fractal geometry of nature*. Freeman, New York
- Mandelbrot BB, van Ness JW (1968) Fractional Brownian motions, fractional noises and applications. *SIAM Rev* 10: 422–437
- Montroll EW, Lebowitz JL (eds) (1987) *Fluctuation phenomena*. Elsevier North-Holland, Amsterdam New York
- Moore SP, Rushmer DS, Windus SL, Nashner LM (1988) Human automatic postural responses: responses to horizontal perturbations of stance in multiple directions. *Exp Brain Res* 73: 648–658
- Nashner LM (1971) A model describing vestibular detection of body sway motion. *Acta Otolaryngol* 72: 429–436
- Nashner LM (1972) Vestibular postural control model. *Kybernetik* 10: 106–110
- Nashner LM (1977) Fixed patterns of rapid postural responses among leg muscles during stance. *Exp Brain Res* 30: 13–24
- Norré ME, Forrez G, Beckers A (1987) Posturography measuring instability in vestibular dysfunction in the elderly. *Age Ageing* 16: 89–93
- Peretto P (1984) Collective properties of neural networks: a statistical physics approach. *Biol Cybern* 50: 51–62
- Saupe D (1988) Algorithms for random fractals. In: Peitgen H-O, Saupe D (eds) *The science of fractal images*. Springer-Verlag, Berlin Heidelberg New York, pp 71–136
- Shlesinger MF, West BJ (eds) (1984) *Random walks and their applications in the physical and biological sciences*. American Institute of Physics, New York
- Shrout PE, Fleiss JL (1979) Intraclass correlations: uses in assessing rater reliability. *Psych Bull* 86: 420–428
- Sompolinsky H (1988) Statistical mechanics of neural networks. *Phys Today* Dec 70–80
- Tuckwell HC (1989) *Stochastic processes in the neurosciences*. SIAM, Philadelphia
- Voss RF (1988) Fractals in nature: from characterization to simulation. In: Peitgen H-O, Saupe D (eds) *The science of fractal images*. Springer-Verlag, Berlin Heidelberg New York, pp 21–70
- Woollacott MH, von Hosten C, Rösblad B (1988) Relation between muscle response onset and body segmental movements during postural perturbations in humans. *Exp Brain Res* 72: 593–604